LOW CYCLE FATIGUE AND POST FATIGUE TENSILE BEHAVIOR OF A NON-CONVENTIONAL AUSTENITIC STAINLESS STEEL

A THESIS SUBMITTED IN PARTIAL FULFILMENT OF THE

REQUIREMENTS FOR THE DEGREE OF

Master of Technology

In

Mechanical Engineering
[Specialization: Steel Technology]

Submitted By:

Supriya Upadhyay

Roll No- 212MM2341

Under Supervision of

Prof. K. Dutta

Department of Metallurgical and Materials Engineering
National Institute of Technology
Rourkela

May 2014

National Institute of Technology

Rourkela

Certificate

This is to certify that the thesis entitled, **"Low cycle fatigue and post fatigue tensile behavior of a Non-conventional austenitic stainless steel"** submitted by **Supriya Upadhyay** in partial fulfillment of the requirements for the award of the degree of **Master of Technology** in **Mechanical Engineering** at the **National Institute of Technology, Rourkela** (Specialization: Steel Technology**)** is an authentic work carried out by her under my supervision and guidance.

To the best of my knowledge, the matter embodied in the thesis has not been submitted to any other University/ Institute for the award of any degree or diploma.

Date:

Place: Rourkela

Supervisor:

Prof. K. Dutta
Department of Metallurgical and Materials Engineering
National institute of Technology, Rourkela-769008.

Acknowledgements

I take this opportunity to express my deep sense of gratitude and respect to my supervisor, Prof. Professor K. Dutta, Metallurgical and Materials Engineering Department, NIT Rourkela, for his inspiring guidance, valuable suggestions, and stimulating discussions throughout the research work. It would have not been possible for me to bring out this thesis without his help and constant encouragement.

I am sincerely thankful to Dr. B.B. Verma, professor Metallurgical and Materials Engineering Department, NIT Rourkela, and other faculty members of this department for their persistent support and advice during the course work.

I am highly grateful to laboratory members of Department of Metallurgical and Materials Engineering, NIT Rourkela, specially Mr. Hembram, Mr. U.K. Sahu, Mr. A. Pal and Mr. K. Tanty and I also like to thanks my friends Hemant and Om prakash for their help during execution of experiment.

I am thankful to all my classmates and friends who made my stay in Rourkela, an unforgettable and rewarding experience.

Finally, I feel great reverence for all my family members and the Almighty, for their blessings, and for being a constant source of encouragement.

Place: Rourkela

Supriya Upadhyay

Contents

Abstract

Traditionally, stainless steels find a wide range of applications, which include pipelines, automobiles, engine and gear parts etc. In many of these applications, structures and components go through fatigue loading ranging for low cycle to high cycle. ISO/TR 15510 X12CrMnNiN17-7-5 is a special grade of austenitic stainless steel, which is developed to conserve nickel and is used in automobile parts such as automotive trim, automobile wheel covers, flat conveyer chains, railroad passenger car bodies. The aim of this project is to explore the low cycle fatigue behavior and its effect on the tensile properties of the abovementioned non-conventional stainless steel, which is unavailable in literature. Attempts have also been made to understand the microstructural variation due to deformation in the steel, as the structure is austenitic, hence metastable in nature. For these purposes a set of non-conventional austenitic stainless steel rods were annealed by soaking at 1000°C for one hour these were followed by water quenching prior to machining.The fatigue studies have been carried out at four different strain amplitudes (at ambient temperature) up to 100 cycles, which have been followed by tensile tests on the fatigued samples at constant crosshead speed of 1mm/minute.

The low cycle fatigue results include that the steel undergoes cyclic softening behavior, which has also been reflected from the post-fatigue tensile results X-ray diffraction studies indicate that deformation induced phase transformation takes place in the steel due to combined effects of fatigue and tensile loading. The extent of phase transformation has been estimated and is correlated with the extent of deformation.

Key Words:
Low cycle fatigue (LCF), Mechanical behavior, Stainless steel, Deformation-induced martensite, Strain amplitude.

List of Figures

List of Tables

CHAPTER 1

INTRODUCTION

Introduction

Fatigue is one of the most crucial criteria, which affect the structure and its components. Damage to a structure does not always occur in one strike. Sometimes load on a particular section of a structure repeatedly results in fracture of the structure at that point. When a load is applied to a particular point of a structure many times of a cycle than the amount of load the other points on the structure are bearing then it results to failure of that structure at that particular point. Sometimes the fracture in the cycle occurs after a few strokes and sometimes it takes more strokes. The fracture occurring in few cyclic strokes is known as low cycle fatigue whereas the one occurring in many cyclic strokes is known as high cycle fatigue [1].

When a fracture is done in a structure then load striking that point repeatedly increases the fracture. This is known as fatigue crack growth (FCG). The number of cycles that are required to initiate a crack in beginning is known as fatigue initiation life. The number of further cycles that are required from the initiation to complete failure of the structure is known as fatigue propagation life.

The factors affecting the fatigue in any structure is not confined only on the criteria of cyclic loads and temperature. Many more criteria's affect in the failure of a structure due to fatigue. The criteria's involves-

- Oxidized environment
- Structural Changes
- Strain holding time of the structure
- Frequency with which the load is applied cyclically

These criteria's make it tough to understand that which one of the criteria is most dominant in understanding the criteria is mostly responsible for causing fatigue.

Many studies have been done in recent years on the elevated temperature, low cycle fatigue properties of various engineering materials.[2]They have revealed that the fatigue life not only depends on strain range and temperature but also on factors such as frequency, strain rate or strain hold time [3]effects of creep damage [4], oxidation environment [5]. Cyclic deformation behavior [6], structural change [7].and so on. Therefore, it is not yet clear which factors are dominant in explaining the low-cycle fatigue behavior for each test condition. It remains difficult; to understand the low cycle fatigue behaviors of metals, since the effect of these factors seems to be very complicated. Therefore, these investigations are done on low cycle fatigue tests to examine its behavior under constant strain amplitude on selected material at ambient temperature condition.

Austenitic stainless steel have Face centered cubic (FCC) lattice structure. They are non-magnetic stainless steels that contain high levels of chromium and nickel, and low levels of carbon. Known for their formability and resistance to corrosion, austenitic are the most widely used grade of stainless steel. They usually possess excellent cryogenic properties, good high-temperature strength, and oxidation resistance. ISO/TR 15510 X12CrMnNiN17-7-5 is a special grade of austenitic stainless steel .This is a non-conventional austenitic stainless steel that was developed to conserve nickel and is used in automobile parts such as automotive trim, automobile wheel covers, flat conveyer chains, railroad passenger car bodies.During deformation of austenitic stainless steel, austenite transforms to martensite [8]; and the structure of this stainless steel is known to be metastable. Therefore the results obtain by these experiments on post fatigue tensile behavior of X12CrMnNiN17-7-5 stainless steel and corresponding micro structural variation would be helpful to improve the fatigue database.

In brief, this investigation incorporates to study on low cycle fatigue and post fatigue tensile behavior and its affect on microstructure variation and mechanical properties of X12CrMnNiN17-7-5 stainless steel.

1.1Objectives of the work

Main objectives of this investigation and plans of work can be briefly summarized as:

(1) To characterize microstructures and to determine related mechanical properties of the selected steel:

This part consists of (a) micro structural characterization of the material, (b) measurement of grain size and, (c) determination of hardness.

(2) To study the low cycle fatigue behavior of the selected steel at different strain amplitude:

The major experiments to fulfill this objective are investigations related to low cyclic fatigue tests under various constant strain amplitudes in order to examine the response of stress (whether cyclic hardening or softening) due to cyclic loading at ambient temperature.

(3) To examine the effect of pre-fatigue cycling on the tensile properties of the selected steel:

The tests in this part include conducting tensile tests on specimens subjected to previous cyclic loading.

(4) To assess the extent of phase transformation due to deformation:

This part consists of microstructural characterization of the deformed material using X-ray diffraction profile analysis.

This thesis is contains total five chapters:

Chapter-1 Introduction and cause of fatigue failure. A brief introduction of parameters, which affect on low cycle fatigue (LCF) behavior of materials during cyclic loading. General concept of micro structural variation of Austenitic stainless steel due to tensile deformation.Significance of the problem and the motivation behind this investigation is discussed in this chapter.

Chaper-2 Gives a critical review of the existing literature in this field.

Chapter-3 Description of experiments procedures, which are being carried out in this Investigation.

Chapter-4 Includes results and discussion of the present work.

Chapter-5 Contains brief discussion and major conclusions of these investigations. Some proposed future works related to this area has been compiled; at the end of this chapter, the references cited throughout the thesis are enlisted.

CHAPTER 2

LITERATURE REVIEW

2.1 The History of Fatigue

Thought it seems very obvious that repeated bending of a piece of wood or metal, back and forth, with large amplitude will cause to break it; however it was a surprising discovery to know that repeated loading also produces fracture even when the stress amplitude is well below the elastic limit of the material. Such of this kind of investigations is first seems to have been reported by a German mining engineer, W.A.S. Albert, who is 1829, performed some repeated loading tests on iron chain. Examples of such fatigues can be dated back to, in the use of axles of stagecoaches. It became a widespread problem when railway systems began to develop rapidly in the middle of nineteenth century, and from here attention to cycle loading effects started. Attempts were made to reproduce these kind of failures in the laboratory, as is often case with unexplained service failures. Between 1852 and 1870, another German engineer August Wohler setup and conducted the first systematic fatigue investigation. He may be regarded as the grandfather of modern fatigue thinking. Some of Wöhler's data are for Krupp axle steel and are plotted, in terms of nominal stress (S) vs. number of cycles to failure (N), on what has become known as the S-N diagram. Each curve on such a diagram is still referred to as a Wöhler line. [9].

2.2 Concept of Fatigue

The primary damage mechanism of structural components is fatigue cracking. It results mainly because of cyclic stresses that are below the ultimate tensile stress, or even the yield stress of the material. The concept of "**fatigue**" tells that a material becomes "tired" and fails at when is reaches below the nominal strength of the material. The original bulk design strengths are not exceeded actually and the warning sign of an impending fracture is not sufficient and even hard to see crack, which leads to fatigue damage more dangerous. The number of loading cycles required to initiate a fatigue crack and to

propagate the crack to critical size can is termed as fatigue life of a component. Fatigue failure occurs in three stages crack initiation; slow stable crack growth; swift fracture [10].

On a single application of load, it will fail at a stress much lower than that required to cause fracture, if a metal is subjected to a repetitive or fluctuating stress. Fatigue failure occurs mainly under conditions of dynamic loading, according to observation, these type of failures occur only after a substantial period of service. The vast majority of structural and mechanical element is subjected to repeated loading for many cycles, termed cyclic loading. The examples of members and structures subjected to cyclic loading are: building and bridges under earthquake and wind-induced forces, aircraft, ships, steam or gas turbine blades, offshore platforms etc. It is well accepted today that all most 90 percent of the all service failure occur due to fatigue [11].

2.3 Types of Loading

Fluctuating stresses are classified into many types. The more common types encountered are shown in figures given bellow.

In figure 2.1 a fully reversed stress cycle is shown, in which maximum and minimum stresses are equal, and is commonly used in testing [12].

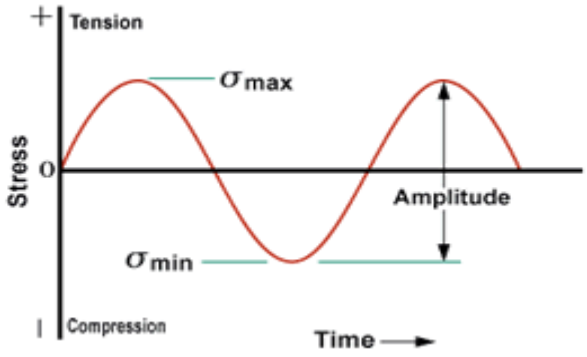

Fig.2.1 Reversed stress cycle.

Repeated stress cycle is the common stress cycle, mean stress (σ_m) applied on top of the minimum stresses. shown in figure 2.2 the condition where both stresses (cyclic and applied) are tensile (greater than zero),It is also feasible to test with both stresses in compression[1].

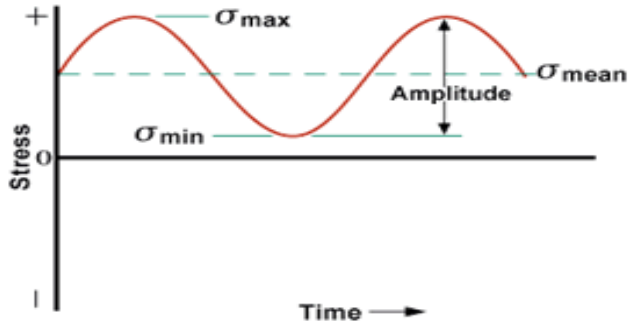

Fig.2.2 Repeated stress cycle.

Furthermore, it is not necessary that the maximum and minimum stresses in the cycle have to be equal in value.

The final type of loading cycle is the random or irregular stress cycle, in which during service the part is subjected to random loads , as shown in figure 2.3[1].

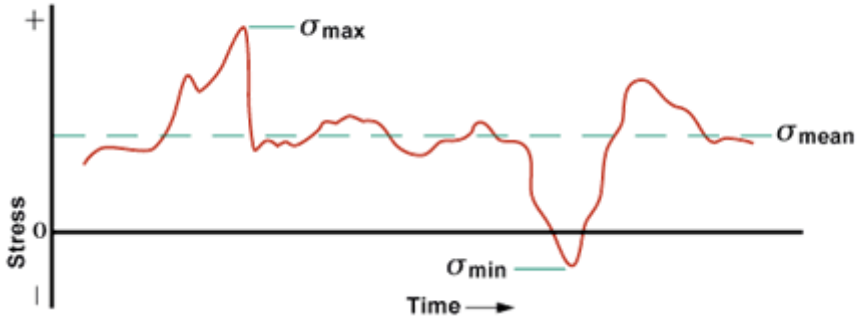

Fig.2.3 Irregular and random stress cycle.

A fluctuating stress comprised of two components:

A mean or steady stress, σ_m, and an alternating or variable stress, σ_a.

The stress range, σ_r, is the difference between the maximum and minimum stress in a cycle:

$$\sigma_r = \sigma_{max} - \sigma_{min} \tag{2.1}$$

The alternating stress (Stress amplitude) is one-half the stress range:

$$\sigma_a = \frac{\sigma_r}{2} = \frac{\sigma_{max} - \sigma_{min}}{2} \tag{2.2}$$

The mean stress is the algebraic average of the maximum and minimum stress in the cycle:

$$\sigma_m = \frac{\sigma_{max} + \sigma_{min}}{2} \tag{2.3}$$

Two ratios frequently used in presenting fatigue data are:

$$\text{Stress ratio} \qquad R = \frac{\sigma_{min}}{\sigma_{max}} \tag{2.4}$$

$$\text{Amplitude ratio} \qquad A = \frac{\sigma_a}{\sigma_m} = \frac{1-R}{1+R} \tag{2.5}$$

2.4 High cycle fatigue and Low cycle fatigue

High-cycle fatigue—where stresses and strains are mainly restricted to the elastic region. High-cycle fatigue is related with low loads and long life. The Stress-Life (S-N) or Total Life procedure is extensively used for high-cycle fatigue approach —here the applied stress is within the elastic range of the material and the number of cycles to failure is large. [13].

Low-cycle fatigue—where significant plastic straining occurs. Low-cycle fatigue involves large cycles with significant amounts of plastic deformation and relatively short life. The analytical procedure used to address strain-controlled fatigue is commonly referred to as the Strain-Life, Crack-Initiation, or Critical Location approach.

While low-cycle fatigue is typically related with fatigue life between 10 to 10^5cycles, high-cycle fatigue is related with life greater than 10^5cycle.to analyze both high-cycle fatigue and low-cycle fatigue, a number of methods have been developed by combining the Manson-Coffin mode[14-16] and Basquin model [14,17].

2.4.1 High cycle fatigue

High cycle fatigue could be sub-divided into-

- High cycle fatigue (HCF) – between 10^5 and 10^7
- Very low life cycles VHCF) – over 10^7 cycles to failure[18].

The VHCF of materials is a phenomenon that first became acknowledged and evoked scientific interest only a few decades ago[19]. It was observed that some materials when subjected to a sufficiently high number of load cycles ($10^8 – 10^{10}$) fail at stress levels that traditionally were considered as safe. Prior to this, it was believed that if a material survives $10^6 – 10^7$ load cycles than it would never fail with increasing number of cycles at the same stress level.

High cycle fatigue must consider during design of automobiles, aircraft, compressors, pumps, turbines etc. where vibration occur. High-cycle fatigue data are generally introduced by a plot of stress, S, versus the number of cycles to failure, N. A log scale is associated with the number of cycles. The value of stress, S, can be the maximum stress, σ_{max}, the minimum stress, σ_{min}, or the stress amplitude, σ_a. The S-N relationship is generally determined for a describe for the value of the mean stress, σ_m, or one of the two ratios, stress ratio or amplitude ratio.

For determinations of the S-N curve, the usual procedure is to test the first specimen at a high stress where failure is expected in a short number of cycles, e.g., at about two-thirds the static tensile strength of the material. The test stress is decreased for each succeeding specimen until one or two specimens do not fail in the specified numbers of cycles, which is usually at least 10^7cycles. This method used for presenting fatigue failure in high cycles ($N > 10^5$).

The number of cycle to failure at a identified stress level is referred as fatigue life , while the fatigue strength (also mentioned as the endurance limit) is the stress below which failure does not occur. As the applied stress level decreases, the number of cycles to failure increases. Normally, the fatigue strength increases as the static tensile strength increases. To the contrary, non-ferrous systems, particularly aluminum and aluminum-based alloys do not possess any well-defined level of stress below which these materials do not fail and therefore, it is critical to define endurance limit for non-ferrous systems. This curve is used to predict the number of cycles sustained under certain stress before failure. The curve gives designers a quick reference of the allowable stress level for an intended service life given bellow in figure 2.4[13].

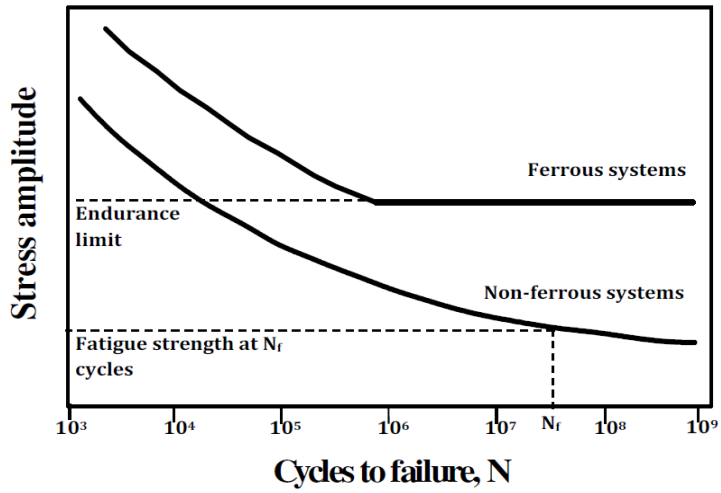

Fig.2.4 Schematic representation of the S-N curve.

2.4.2 Low cycle curve

Low cycle fatigue could be also sub-divided into-

- Low cycle fatigue (LCF)– for less than 10^4 cycles to failure.
- Very low life cycles - for less than 100 cycles to failure.

The very low cycle regime is well-known now and is titled as ‘‘extremely low cycle fatigue” (ELCF)) [20-23] to differentiate from the linear part of the life cycle curve that fits the Manson–Coffin law, which occasionally introduced as the ‘‘low cycle fatigue” in a more exact sense. The failure approaches are also dissimilar in these two regimes. For example, in push–pull fatigue tests of cylindrical bars, the fracture in the ELCF range often occurs at the center of the cylindrical bar; while in the strict LCF regime, the crack often starts from the surface[21,24]. Efforts have been made to control the disadvantage of Manson– Coffin law in the ELCF regime, e.g. Hatanaka et al [25] Kuroda [26] and Tateishi et al [27] More recently, Chen et al. derived a power exponential relationship by raising the logarithm of the plastic strain amplitude to a non-unity power and showed good agreement with experimental data [28].

Low cycle fatigue is the repeated cyclic loadings that cause remarkable plastic distortion in a material. Low cycle fatigue generally occurs because of repeated localized yielding near stress raisers, such as holes, fillets, and notches, despite the elastic deformation occurring over the bulk of the component. Uniaxial testing is performed on several smooth (unnotched) specimens under different cyclic deformation levels in a typical low cycle fatigue test. The mode of testing is strain control instead of stress control. Stress response monitored during cyclic loading, and the number of cycles to failure is recorded for these tests. The results from several tests are necessary to determine the cyclic stress-strain curve and the strain life curve figure 2.5.

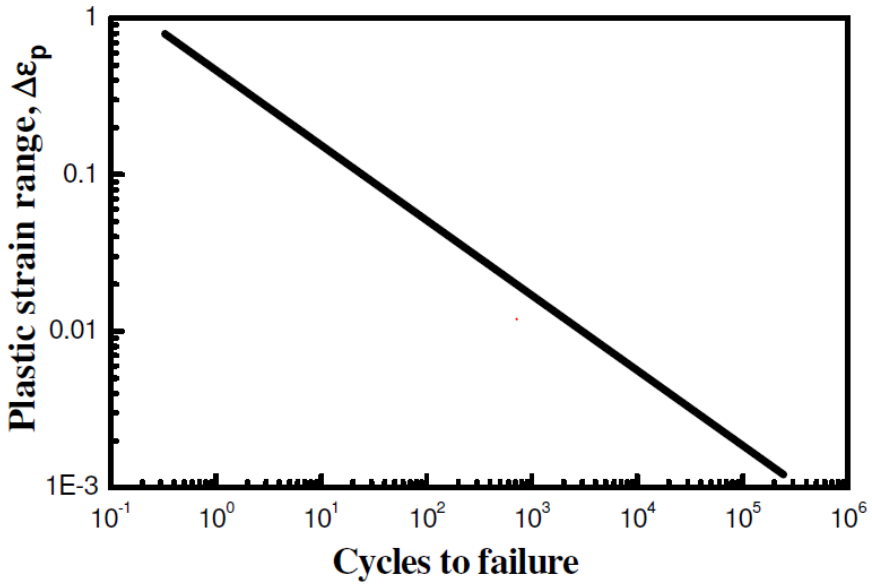

Fig.2.5 Low cycle fatigue curve ($\Delta\varepsilon_p$vs. N).

2.5 Fatigue Strain-Life Relationship

Antecedent studies by Tong et al. (1989) and Lefebvre and Ellyin (1984) have indicated that for fully reversed constant-strain-controlled test, there is negligible variation in the cyclic hysteresis energy with the number of cycles during fatigue life. As shown in figure bellow the hysteresis energy of the cycle at half-life can be used as a characteristic of the entire test (Mander et al., 1994)[29].

Under the cyclic loading within elastic region, stress is directly propositional to strain through modulus of elasticity. However, plastic strains which is produced by cyclic loading, and responses are more complicated and create a hysteresis loop in figure 2.6 [30] from the point O to the point A, the section is in tension. On removing of the load the strain, reaction of the specimen comes after in order to the curve from A to the D. At D, the section is under no stress. As the specimen is subjected to compressive stress, the strain reaction come after in order the curve from D to the point B. delivering the compressive

Stress from B and reapplying the tensile stress, the specimen stress-strain condition come back to the point A along the curve explain by B, C, and A. Points A and B represent the cyclic stress and strain limits. The total strain σ_e, consists of both elastic and plastic components:

$$\Delta\varepsilon = \Delta\varepsilon_e + \Delta\varepsilon_p \tag{2.6}$$

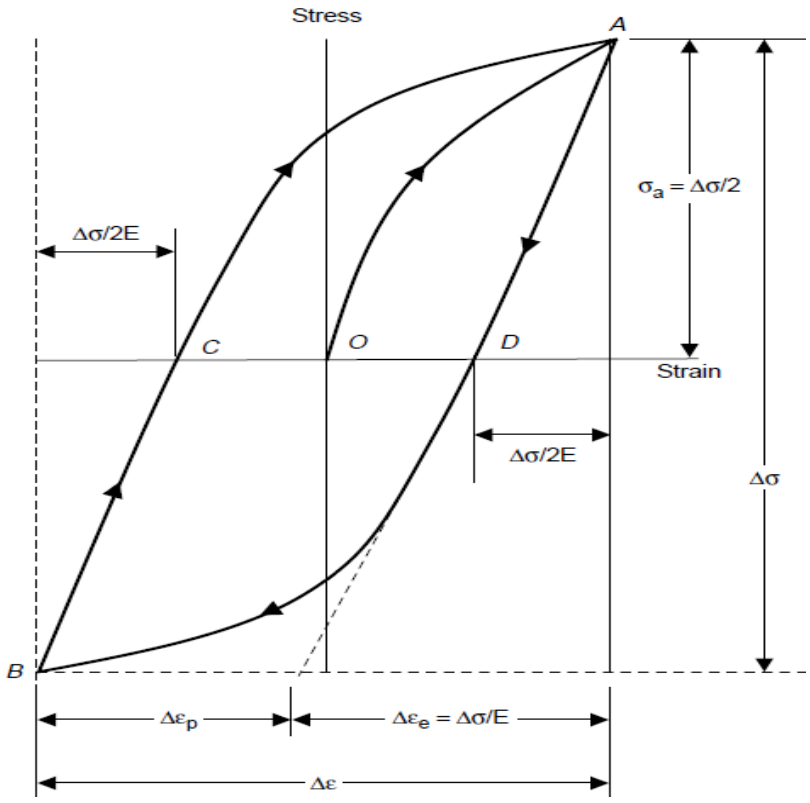

Fig. 2.6:stable cyclic stress versus strain hysteresis loop (Stephens et al., 2001)

where $\Delta\varepsilon_e$ is the elastic strain and $\Delta\varepsilon_e=\sigma_s/E$, and $\Delta\varepsilon_p$is the plastic strain and $\Delta\varepsilon_p$ is the width of the loop at its center, i.e., the distance CD in figure 2.6The area of the hysteresis loop is equal to the energy loss or the work done per cycle.

Low-cycle fatigue test data are commonly shows as a plot of the plastic strain range, $\Delta\varepsilon_p$, versus cycles to failure, N. When plotted on log-log coordinates, a straight line is obtained that is described by the Coffin-Manson relation:

$$\frac{\Delta\varepsilon_p}{2} = \varepsilon'_f(2N)^c \tag{2.7}$$

where$\Delta\varepsilon_p$=2 is the plastic strain amplitude, and $\acute{\varepsilon}_f$ is the fatigue ductility coefficient defined by the strain intercept at 2N=1. For many metals, $\acute{\varepsilon}_f$ roughly equal to the true fracture strain, ε_f. 2N is the number of strain turnaround to failure, and c is the fatigue ductility exponent, which is usually varies between -0.5 and - 0.7. A smaller value of c results in longer fatigue lives.

The Basquin equation, which describes the high-cycle fatigue , low-strain regime where the nominal strains are elastic, is:

$$\sigma_a = \frac{\Delta\varepsilon_e}{2}E = \sigma'_f(2N)^b \tag{2.8}$$

Where: σ_a is the alternating stress amplitude,

$\Delta\varepsilon_e$=2 is the elastic strain amplitude, E is the young's modulus, and σ'_f is the fatigue strength coefficient, expressed as the stress intercept at 2N=1. σ'_f is roughly requal to the true fracture stress, σ_f. 2N is the number of load turnaround to failure, and b is the fatigue strength exponent, which varies for most metals between -0.05 and -0.12. A smaller b results in a longer fatigue life. Combining Basquin's equation and the Coffin-Manson equation gives an equation that can be used to estimate the entire range of fatigue lives:[30].

$$\frac{\Delta\varepsilon}{2} = \frac{\Delta\varepsilon_e}{2} + \frac{\Delta\varepsilon_p}{2} \tag{2.9}$$

$$\frac{\Delta\varepsilon}{2} = \frac{\sigma'_f}{E}(2N)^b + \varepsilon'_f(2N)^c \tag{2.10}$$

For high-cycle strain conditions, ductile metals have the longest lives, while at low-cycle strain conditions; strong metals have the longest lives.

2.6 Fatigue strain-life curve

The fatigue strain-life curve tends toward the plastic curve at large strain amplitudes and toward the elastic curve at small strain amplitudes figure 2.7 For high-cycle strain conditions, ductile metals have the longest lives, while at low-cycle strain conditions; strong metals have the longest lives[30].

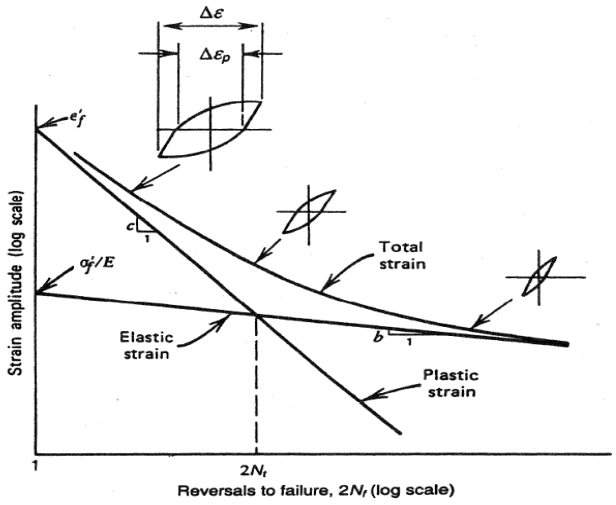

Fig. 2.7: strain-life curve Shows total, elastic, and plastic strain Components (Stephens et al., 2001)

[

2.7 Effect of mean stress on Fatigue

The response of mean stress on stress amplitude to be forecast from fully reversed-bending data ground on a number of mathematical models. Goodman developed a linear model, while Gerber used a parabolic model figure 2.8 test data for ductile metals that generally fall closer to the Gerber's parabolic nature of curve. However, the scatter in fatigue data and the fact that notched data fall adjacent to the Goodman line, the more conservative Goodman relationship is frequently used in practice. If the design of component is ground on yield rather than ultimate strength, as most are, then the even more conservative Soderberg relationship can be used. Mathematically, the three relationships can be demonstrated as:

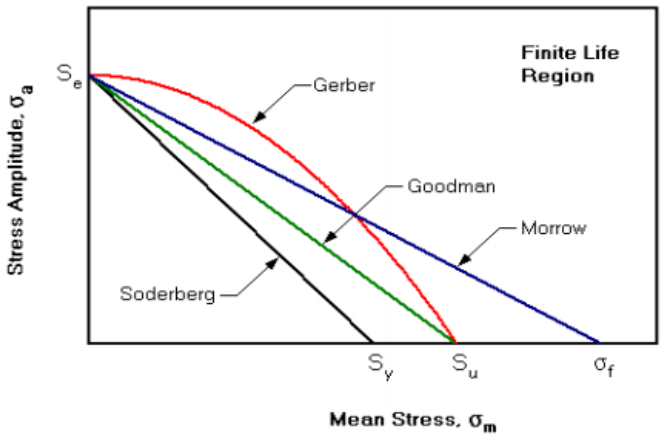

Fig. 2.8: Effect of mean stress on alternating stress amplitude.

Soderberg (USA, 1930) $\sigma_a/\sigma'_e + \sigma_m/\sigma_y = 1$ (2.11)

Goodman (England, 1899) $\sigma_a/\sigma'_e + \sigma_m/\sigma_u = 1$ (2.12)

Gerber (Germany, 1874) $\sigma_a/\sigma'_e + (\sigma_m/\sigma_u)^2 = 1$ (2.13)

Where

σ_a = Stress amplitude.

σ_m =Mean stress

σ_y =Yield stress

σ_u = Ultimate tensile stress

In general, all are the relationships show that with increase in mean stress the alternating stress amplitude required for fatigue endurance limit gradually decreases. The Goodman relation gives good results for brittle materials and conservative results for ductile materials. The Gerber relation gives good results for ductile material. Fatigue strength of a component tends to be increasing with a compressive mean stress and decreasing with a tensile mean stress. Gerber's parabolic relationship may therefore yield erroneous answer to the conservative side in the compressive mean stress region.

2.8 Cyclic hardening and softening

The stress response and physical properties of material changes with micro structural changes due to cyclic loading application .Cyclic softening / hardening effect associated to softening/hardening of material's response to decreasing/increasing of resistance against material deformation under cyclic loading Its intensity usually decreased with number of cycles until the saturated state is reached. During uniaxial cyclic loading, the condition is characterized by closed hysteresis loop. Transient responses in initial cycles caused by cyclic hardening/softening under plastic strain control and stress control as shows in the figure 2.9 [31].

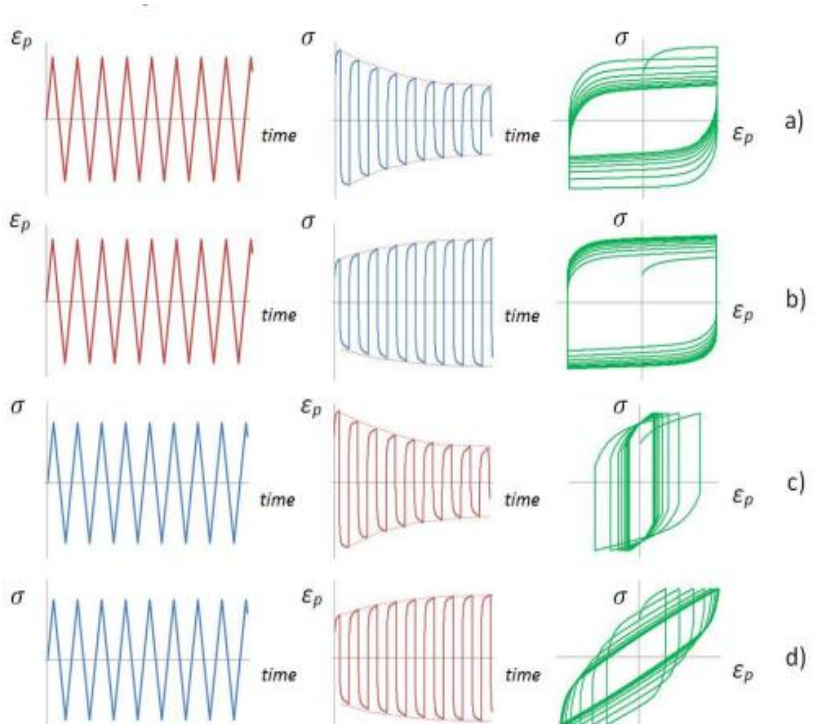

Fig. 2.9: Uniaxial fatigue test material response: Cyclic softening **a)** and cyclic hardening **b)** under plastic strain controlled loading, and under stress controlled loading:Cyclic softening **c)** and cyclic hardening **d)**

Cyclic softening and cyclic hardening are different for different types of materials like Some materials shows very strong cyclic softening/hardening like as stainless steels, cooper, etc. some less obvious (structural steels).There are also extraordinary cyclic hardening in certain cycles range and in the remaining lifetime cyclical softening. Properties of cyclic hardening and softening do not depend only on material microstructure, but also on loading amplitude or more u on previous strain history.[31].

For the unstable behavior of materials it is difficult to makes exact stress-strain modeling. There is very often mentioned possibility of unstable stress-strain behavior estimation

according to its strength limit and yield limit ratio, but also very simple hypothesis is used, claiming that hard material cyclically softens whereas soft material cyclically hardens.

2.9 Tensile properties

Tensile properties determination is how the material reacts against the force being applied in the tension. It is a fundamental mechanical test for which a carefully prepared specimen needs to be loaded in a very controlled manner. While measuring the applied load and the elongation of the specimen over some distance. Tensile tests are used to determine the elastic limit, modulus of elasticity, proportional limit, elongation, and reduction in area, yield point, tensile strength, yield strength and other tensile properties

The main purpose of the tensile test is to determine the load –elongation curve, stress and strain are obtained, by dividing the load and elongation by constant values from which stress versus strain relation are obtained both the curve are same shaped .The stress-strain curve relates the applied stress to the resulting strain and each material has its own unique stress-strain curve. A typical stress-strain curve shown below in figure.2.10.[32].

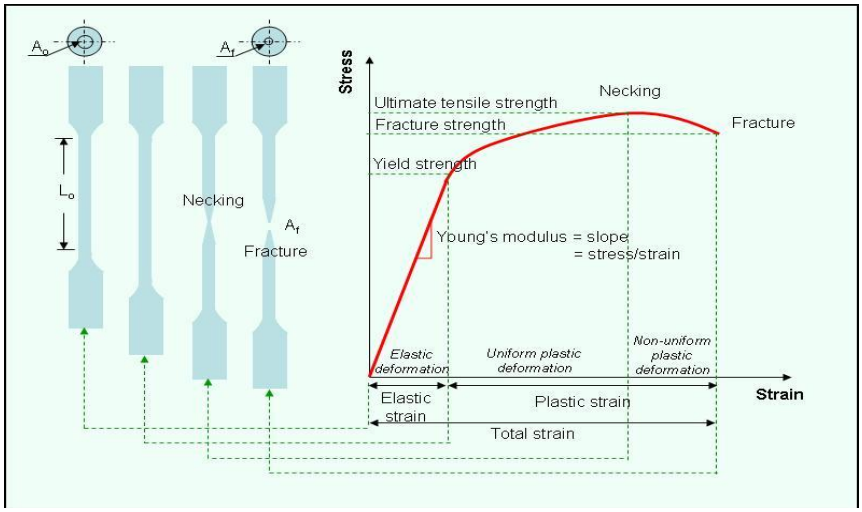

Fig. 2.10: A typical engineering stress-strain curve during tensile test.

2.10 Materials on which Low cycle fatigue behavior have been studied

There are various materials on which low cycle fatigue tests have been conducted such as 304L austenitic stainless steel, carbon steel, stainless steel types 347N and 316N, eutectic solder alloy, mild steel. Baglion et al. [33], has been studied on 304L austenitic stainless steel in air / in vacuum, at 20°C or at 300°C: relative effect of strain rate and environment which shows that strain amplitudes a decreased in stress levels when the temperature is increased from 20 to 300°C and it also exhibits secondary hardening in certain conditions of temperature and strain amplitude. That behavior was also observed in type 316L stainless steel by Gerland et al. [34]. Jun Oh et al. [35] have been studied on stainless steel types 347N and 316N. For comparison of both of them which shows that the cyclic response of type 347N stainless steel exhibits strong secondary cyclic hardening till the final failure at ambient temperature but in case type 316N stainless steel ,did not exhibit secondary hardening behavior. Srinivasan V.S. [36] has also investigated 316N stainless steel at low fatigue tensile behavior at high temperature, which results shows that the material exhibits an initial hardening followed by a saturated stress response before the final load drop associated with the initiation and propagation of fatigue cracks. In addition, the response of Negative strain rate stress at 773 K and 823 K, i.e. an increase in cyclic stress response with decrease in strain rate from 3×10^{-2} s^{-1} to 3×10^{-5} s^{-1}. This shows that low cycle fatigue behavior affected by strain rate and temperature at which experiments are performed. This experiment has done to determine the cyclic response of austenitic stainless steel due to various strain rates and strain amplitude.

2.11 Deformation of austenite in to martensite and quantitative estimation of volume fraction due formation of martensite:

For industrial application austenitic stainless steels are extensively used material there the control of its microstructure evolution, physical and mechanical properties are important

factors. It is well known that such kinds of materials plastic deformation can induce transformation of austenite into martensite. According to Perdahciogˇlu*etal*.the initiation of transformation will always be from a virgin 100% austenite material [37]

The sequence of deformation of austenite stainless steel in to maetensite is:

Austenite γ(FCC)→Martensiteε (HCP)→Martensite ά (bCC)

There are two different types of martensite can be formed by this mechanism: ε martensite, a paramagnetic phase (just as the austenite), bearing hexagonal close packed (hcp) structure, and α' martensite, ferromagnetic, body centered cubic (bcc) with the same crystallographic lattice parameters of ferrite phase [37] The amount of martensite deformation depends upon various factors such as: material chemistry, temperature, plastic strain, strain rate, stress state, deformation mode, grain size, grain orientation, etc. Eichelman and Hull had developed an equation which gives an approximation of a'martensite formation temperature – Ms:

Ms (ºC) = 1302 – 42(% Cr) – 61(% ni) –33(% mn) – 28(% si) – 1667 (% [C + n]) (2.14)

The energy that is responsible for formation of martensite can be given by plastic deformation process. On the other hand, there is a temperature about which martensite cannot form under deformation, Md. (the temperature below which martensite will form under deformation) Angel et al. have studied the dependence of temperature with composition for different steels and formulated equation [37].

Md(30/50)(°C) = 413 – 13.7(%Cr) –9.5(%ni) – 8.1(%mn) – 18.5(%mo) – 9.2 (%si) – 462 (%[C + n]) (2.15)

Md is the temperature at which 50% of the ά–martensite is produced after 30% true deformation under tensile condition.

During tensile teststhe quantitative estimation of deformed phaseshave been done for tensile deformation by De et al. [38] and this method is described by X-ray diffraction analysis which required for this type of quantification, from which it can be
Stated that total integrated intensity of all diffraction peaks for each phase is proportional to its volume fraction. It can be stated that :

$I_i^{hkl}=CR_i^{hkl}V_i/2\mu$ (2.16)

Where,

$$C=\left(\frac{I_0 A\lambda^3}{32\pi r}\right)\left[\left(\frac{\mu_0}{4\pi}\right)\frac{e^4}{m^2}\right] \quad \text{and,}$$

$$R_{hkl}=\left(\frac{1}{\upsilon^2}\right)\left[|F|^2\ p\left(\frac{1+\cos^2 2\theta}{\sin^2\theta\cos\theta}\right)\right]\left(e^{-2M}\right) \qquad (2.17)$$

The terms uses in these equations are:

$I_i^{hkl:}$ integrated intensity for (hkl) plane of i-phase, i: γ, α';

C: the instrument factor;
R_{hkl}: is the material scattering factor and depends on diffraction angle (θ), interplanar spacing of hkl, composition and crystal structure of phase i;

υ: is the volume of unit cell,
F_{hkl}: is the structure factor for reflecting phase (hkl),

The structure factor is independent of the shape and size of the unit cell.
p: multiplicity factor,

It can be reported as the number of various planes in a form having the same spacing. Parallel planes with various Miller indices, such as(100) and (-100), are counted Individually as different planes, yielding numbers which are double those given in the Antedate paragraph. Thus the multiplicity factor for the {100} planes of a cubic crystal is 6 and for the {111} planes 8.

e^{-2M}: temperature factor.

As the temperature is raised, the intensity of diffracted beam decreases and for constant temperature the thermal vibration causes a greater decrease in the reflected intensity at high angles than at low angles.

λ: the wavelength of incident X-ray beam.

μ: linear absorption coefficient.

A: cross sectional area of incident X-ray beam.

I_0 : intensity of the incident beam.

r: radius of diffract meter circle.

$e^{-}{}^{2m}$: charge and mass of electron.

Therefore, for a steel containing austenite (γ), bcc martensite (α') and hcp-martensite (ε), then Eq. (2.16) may be written as:

$I_\gamma = K R_\gamma V_\gamma / 2\mu$ and

$I_{\alpha'} = K R_{\alpha'} V_{\alpha'} / 2\mu$

Additionally,

$V_\gamma + V_{\alpha'} = 1$ (2.18)

From the above relations, the volume fraction of austenite and martensite can be derived for numerous peaks as [39] where C/2μ is constant in a given X-ray diffraction scan.

$$V_i = \frac{\frac{1}{n}\sum_{j=1}^{n}\frac{I_i^j}{R_i^j}}{\frac{1}{n}\sum_{j=1}^{n}\frac{I_\gamma^j}{R_\gamma^j}+\frac{1}{n}\sum_{j=1}^{n}\frac{I_{\alpha'}^j}{R_{\alpha'}^j}} \qquad (2.19)$$

Where,

i = **γ**, or **α'** in this instance and n is the number of peaks examined.

Eq. (2.19)enables simultaneous calculation of the volume fraction of austenite and **α'**-martensite in non-conventional stainless steel from a single XRD scan.

CHAPTER 3

Experimental

3.1 Introduction

The aim of this investigation is to study of the low cyclic fatigue behavior, post fatigue tensile behavior and associated microstructural deformation of a non-conventional austenitic stainless steel. Experiments were conducted which are described in this chapter. An overview of all the experiments includes determination of chemical composition of the selected steel, heat treatment, microstructural characterization, scanning electron microscopy, determination of tensile behavior of the steel, hardness test, study of facture surfaces, experiments related to low cycle fatigue behavior under various strain amplitudes, determination of phase transformation using X-ray diffraction studies.

3.2 Material Selection

Austenitic stainless steel which is known as X12CrMnNiN17-7-5 according to ISO/TR 15510:1997 [40] was selected for this investigation. This material is commercially pure in nature. It was available in the form of rod with diameter 16 mm.

3.3 Chemical composition

The chemical composition of the selected steel was assessed using optical emission spectrometer (model: ARL 3460 Metals Analyzer, Thermo Electron Corporation Limited, Switzerland).

3.4 Heat Treatment

The pre deformation history of the material was unknown so it was necessary to remove any residual stresses that may present in it.Further, the heat treatment of austenitic stainless steel involves solution annealing, which helps in dissolvingany precipitated carbide phase at high temperature. The precipitated carbides may causelesser corrosion resistance. Solution treatment of the investigated stainless steel was done by heating the steel at 1000°C for 1 hour that was followed by water quenching.

3.5 Metallographyand specimen preparation

Metallography consists of the study of a materials microstructure. Samples about 9 to 10 mm of height were cut from the heat treated rods. This cutting piece of material were grounded roughly on a belt grinder and grinding was done by moving the sample across the surface of the flat belt grinder. During grinding operation, sample was kept cool by repeated dropping into water. After rough grinding, sample was polished by a series of emery papers. Emery papers contain consecutively finer abrasive grains such as grades of 1/0, 2/0, 3/0 and at last 4/0. The sample was moved in perpendicular direction (90 degree's movement) to the existing scratches during each polishing operation. After polishing through the series of emery papers sample was polished by using wet rotating wheel covered with special cloth that was charged with abrasive. Process of polishing was continued until the surface is plane and free of nicks or inflection etc. After polishing sample was carefully cleaned with soap solution, and subsequently dried using drier. These samples were then polished using diamond paste up to 0.25 µm surface finish. The polished specimen was etched with aqua regia solution [75%HCl and 25% HNO_3].

3.5.1 Optical Microscopy

Microstructure of the samples were obtained by optical microscope (Model: Olympus BX61,Tokyo, Japan), and images were captured at different magnifications. Optical microscope has been shown in figure 3.1.

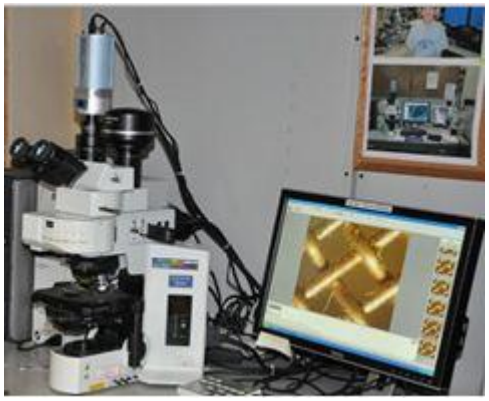

Fig3.1: Image of optical microscope

3.5.2 Grain size Measurement

The average grain size of the investigated steel was determined using liner Intercept method according to ASTM standard E-112 [41].As per the method, a liner test Grid was superimposed on a typical microstructure. Number of stainless steel grains intercepted by the test lines was counted. Such measurements were repeated on 10 randomly chosen fields at a magnification of 100X. The average grain size was anticipated by using the formula:

$d = L_T/N_L$ (3.1)

Where

N_L = Number of grains intercepted by a unit true test line length.

L_T = True length of the test line.

True length of the test line can be defined as the length of the test line at unit magnification.

3.6 Mechanical properties

3.6.1 Hardness Determination

Hardness tests were done by using a Vickers Microhardness Tester (Model: Leco LV 700, USA); the machine is shown in figure 3.2.

Fig.3.2: LecoLV 700 Vickers Microhardness.

To ensure accuracy of measurement, samples were ground flat and parallel to opposite surfaces using belt grinder; followed by mechanical polishing of the sample following the procedures mentioned in section 3.5. Hardness tests were done by using an indentation

load of 5gf. To obtain average hardness at least 3 readings were considered for each sample. Vickers hardness was calculated by using the relations:

$H_v = 1.854P / (d_{avg})^2$ (3.2)

Where: P= applied load in kgf.

$d_{avg} = (d_1+d_2)/2$

Where, d_1 and d_2 are the lengths of two indentation diagonals

.

3.6.2 Tensile properties determination tests

The tensile tests were done at ambient temperature on the cylindrical specimens of gauge length of 25 mm and diameter of 6 mm. All specimens were fabricated from heat treated cylindrical rods of 120 mm initial length and 16 mm initial diameter shown in figure 3.3 according to ASTM standard E-8M [42]. For tensile tests, all the specimens were polished in lathe machine to attend fine surface finish. All tensile tests were carried out using a 100 kN universal servo-hydraulic BISS testing machine (model no. AC 01-0010, Bangalore Integrated Systems Solutions, Bengaluru, India), at a constant cross head speed of 1mm/ min. This crosshead speed corresponds to nominal strain rate of 6.66×10^{-4} s^{-1}. For each test load, displacement signals were automatically recorded, and the digital values of load and displacement were stored in a computer for subsequent processing.

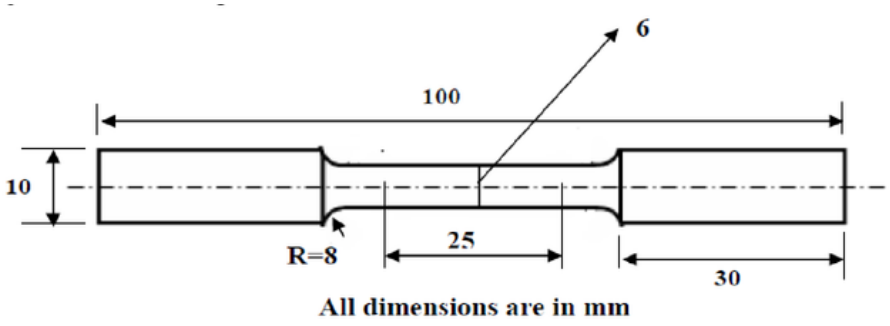

Fig.3.3:A Typical tensile test specimen

3.6.3 Low cycle fatigue tests

Strain controlled low cycle fatigue experiment were carried out at ambient temperature using sevo- hydraulic universal testing machine figure 3.4.

Fig.3.4: universal servo-hydraulic BISS testing machine.

A round bar of non-conventional austenitic stainless steel with diameter of 6 mm and gauge length of 12.5 mm were used for this experiment. The tests were carried out under various constant strain amplitudes at ambient temperature. All these details are listed in Table 3.1. During each test, variation in maximum and minimum stresses with increasing in number of cycles up to 100 cycles of data was continuously recorded by using the attached software to the computer. The test frequency (f) at a certain total strain amplitude could be defined by the following formula, $f = \acute{\varepsilon}/(4\varepsilon_a)$, where ε_a is the total strainamplitude. The incremental step test method was also employed.

Table 3.1 Test Matrix for Low cyclic fatigue tests

Material: **ISO/TR 15510 X12CrMnNiN17-7-5 SS**			
Sample No.	Strain Amplitude (%)	Strain rate (s^{-1})	Frequency (Hz)
1	0.10	$1x10^{-4}$	0.025
2	0.30	$1x10^{-1}$	0.008
3	0.10	$5x10^{-4}$	0.125
4	0.30	$5x10^{-3}$	0.417
5	0.45	$5x10^{-3}$	0.278
6	0.65	$5x10^{-3}$	0.192
7	0.45	$3x10^{-3}$	0.167
8	0.65	$3x10^{-3}$	0.115

3.6.4Post fatigue tensile tests

The samples which were used for low cycle fatigue tests were used to determine post-fatigue tensile properties after low cycle fatigue. The procedure for these tests was same as described in section 3.6.2. The data acquired in data acquisition system are processed to obtain the mechanical properties of the material.

3.7 Fractography

To study the fracture surface, transverse sections from the gauge potion of the broken tensile samples were cut. Fracture surface of the samples were taken by scanning electron microscope (SEM) at different magnifications.

Fig.3.5: Scanning electron microscopy.

3.8 X-ray Diffraction (XRD)

X-ray diffraction is a characterization method for crystalline materials, such as steel. Qualitative and quantitative phase analysis, strain/stress analysis and quantification of preferred orientation (texture) can be performed. A set of fatigue + tensile tested specimen were taken for investigating possible variations in their microstructure. Deformed specimens were cut using a slow speed diamond cutter and these were subjected to X-ray diffraction studies. The XRD (Model: XPert-3040Y00, Holland) analyses were carried out using high-resolution Cu-Kα radiation. Samples were subjected to XRD in the scanning range of 40°- 100° and scanning rate of 2°/min.

CHAPTER 4

Results & Discussions

4.1 Introduction

The aim of this investigation is to study the low cycle fatigue (LCF) behavior of a non-conventional austenitic stainless steel under constant strain amplitude conditions. It was also intended to examine the possible in situ phase transformation of theinvestigated steel during fatigue as well as tensile deformation, as it is known that austenitic stainless steelis metastable up on deformation. For achieving these aims, various experiments have beenconducted, which are described in **chapter3**. This chapter deals with the obtained results ofall the experiments conducted during this investigation in association to their pertinentdiscussion. The chapter is divided into various sub-sections: **Section 4.1** deals with chemicalcomposition of the investigated material; microstructural analyses have been discussed in**Section 4.2**; results of conventional mechanical properties have been provided in **Section 4.3**with relevant discussion, **Sections 4.4** to **4.6** includes results and discussion of low cycle fatigue and post fatigue tensile behavior, in-situ variation of microstructure, fractographic features of the broken tensile sample.

4.2 Chemical composition

Chemical composition of the investigated special grade of non-conventional austenitic stainless steel (X12CrMnNiN17-7-5) was obtained by OES, which is shown in table 4.1. This grade of stainless steel is analogous to X5CrNi17-7 [39].X12CrMnNiN17-7-7 austenitic stainless steels have high ductility, low yield stress and relatively high ultimate tensile strength good corrosion resistance. The major alloying elements of austenitic stainless steels are Cr and Ni approximately in the range of 16-25% and 8-20% respectively with low carbon content [43]. This austenitic stainless steel is having 0.14% carbon with common alloying elements of Ni and Cr as3.66% and 15.6% respectively.

Table 4.1: Chemical composition of the non-conventional stainless steel (all in wt. %).

Material	**Elements**						
ISO/TR 15510 X12CrMnNiN17-7-5 SS	C	Ni	Cr	Mn	Al	Ti	V
	0.14	3.96	15.6	5.49	0.03	0.02	0.06
	Si	S	P	Mo	Cu	N	Fe
	0.53	0.016	0.042	0.21	0.05	0.135	Bal

The steel also contains 5.49% Mn. There are different types of stainless steels: due to addition of nickel for instance, stabilization of the austenite structure of iron occur and by addition of manganese austenitic structure retain m at all temperatures. Manganese preserves an austenitic structure in the steel, as like as nickel, but at a lower piece comparison to nickel. Therefore the presence of Ni or/and Mn is responsible for FCC crystal structure of the steel. As the alloying elements are different as compared to that in conventional 300 series austenitic stainless steel, this steel is referred to as non-conventional austenitic stainless steel [39].

4.3 Micro structural analysis

Optical microstructure of the investigated non-conventional stainless steel reveals that the steel possesses equiaxed austenite grains. Optical micrographs of the non-conventional austenitic stainless steel were taken at various magnifications. A typical micrograph of the investigated stainless steel is shown in Figure 4.1. Grain size is obtained by using linear intercept method according to ASTM standard E112 [44]. Average grain size of the specimen was found to be 50 μm.

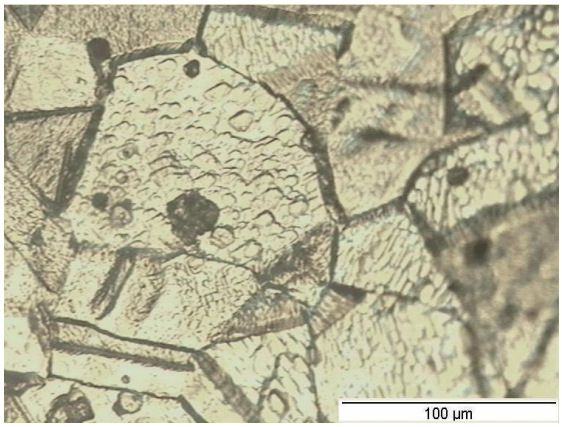

Fig. 4.1: A typical micrograph of investigated stainless steel

4.4 Mechanical properties

Investigated mechanical properties of austenitic stainless steel are included hardness and tensile properties. Microhardness tests of the specimen were carried out by using Vickers microhardness tester and tensile tests were done on servo-hydraulic universal testing machine.

4.4.1 Hardness determination

Micro hardness of the non-conventional austenitic stainless steel samples were taken at different positions of the sample. At least three readings were taken for each sample to obtain average value of Hardness. The results are listed in table 4.2

Table 4.2 Micro hardness values of the non-conventional stainless steel.

Material	**D_1 (µm)**	**D_2 (µm)**	**Hv0.050**	**Average Hv0.050**
ISO/TR 15510 X12CrMnNiN17-7-5 SS	19.30	20.30	236.5	≈228
	19.17	21.13	228.4	
	20.60	21.17	221.6	
	20.24	20.06	216.3	
	19.31	21.23	239.3	
	19.62	21.50	222.3	
	20.08	21.07	214.5	
	19.26	19.95	228	
	19.14	20.60	241.7	
	19.56	20.85	230	

Dwell time for microhardness test is 15 sec, with applied load of 0.05kgf. As per literature, austenitic stainless steels possess hardness ≤253 VHN [45].Current results indicate that the hardness of the investigated steel is ≈228 $Hv_{0.050}$. From Table 4.2 it is clear that hardness of the investigated stainless steel falls under the hardness range of austenitic stainless steel.

4.4.2Tensile Properties

Tensile test is known as a basic and universal engineering test to find the material parameters such as ultimate tensile strength, yield strength, % elongation, % area of reduction and Young's modulus. These parameters plays important role for selection of engineering materials for any required applications. This test is carried out by applying

longitudinal or axial load at a specific extension rate to a standard tensile specimen with known dimensions (gauge length and cross sectional area perpendicular to the load direction) until failure. The plots of stress verses strain are obtained during tensile tests at ambient temperature. The engineering stress-engineering strain graphs for the investigated steel in solution-annealed condition are illustrated in Figure 4.2 (a) while the true stress-true strain curves are shown in Figure 4.2 (b). It can be seen from Figure 4.2 (a) that there is continuous yielding behavior from elastic to plastic regime for the steel and hence the yield strength of the steel is determined using 0.2% strain offset method,according to ASTM standard E8M [42]. The results of tensile experiments are tabulated in Table 4.3. To determine the values of strain hardening exponent (n), true stress (σ) and true strain (e) of investigated material are calculated from the data of engineering stress and engineering strain and the result obtained by the plot of log (true stress) vs. log (true strain) in plastic domain are in straight line as shown in Figure 4.2 (c) and the values of strain hardening exponent (n) are calculated by using Hollomon equation $\sigma=K\varepsilon^n$, where K is strength coefficient [11]. The value of strength coefficient is calculated from the intercept of this plot to the stress axis at $\varepsilon=1$).

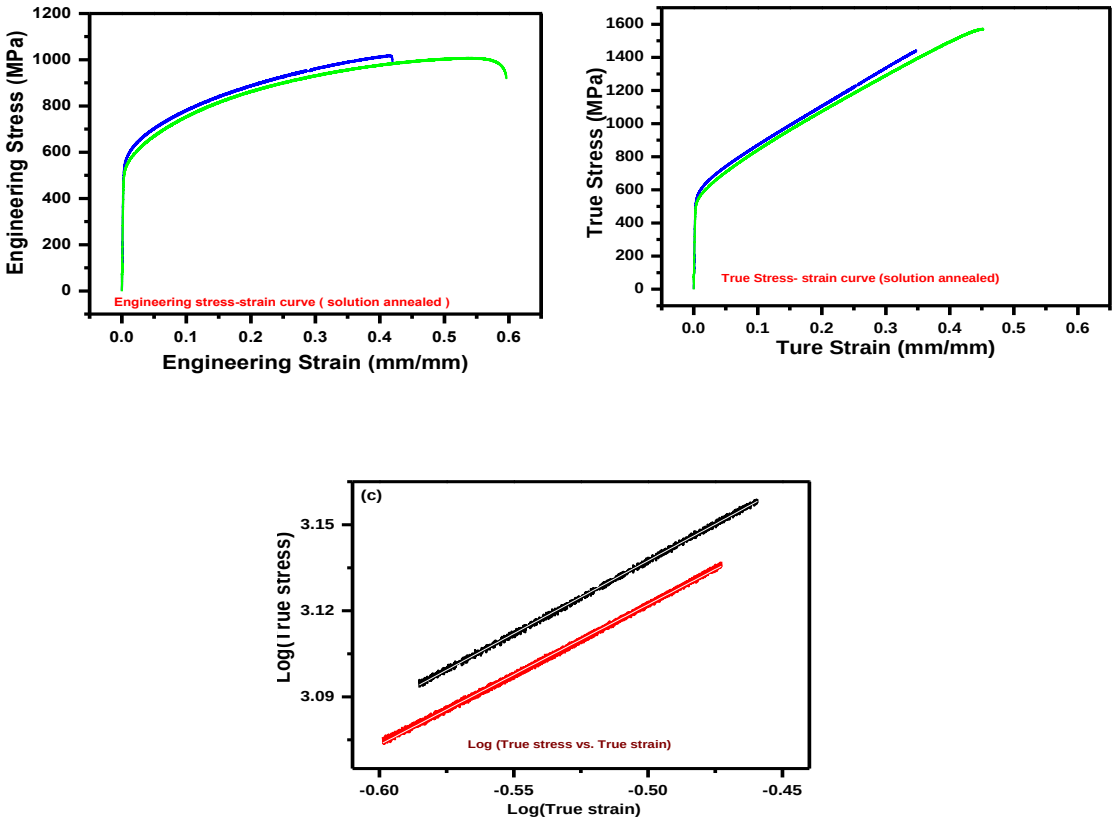

Fig 4.2:(a) Engineering stress-strain behavior, (b) True stress-strain behavior and (c) logarithmic nature of true stress-strain a ,at a constant cross head speed of 1mm/ min corresponds to nominal strain rate of 6.66×10^{-4} s^{-1}.

Table 4.3 Tensile properties of the investigated stainless steel.

Material: ISO/TR 1551 X12CrMnNiN17-7-5 SS					
Sample No.	Yield Strength (MPa)	Ultimate Tensile strength (MPa)	Total elongation% (e_t)	values of strain hardening exponent (*n*)	Values of strength coefficient *(K)* (MPa)
1	545	1020	44.4	0.50877	2494.179
2	521	1008	81.08	0.48908	2418.432

The broken tensile specimens after tensile tests have been subjected to scanning electron microscopy (SEM) to observe the facture surface. A typical fractograph is shown in Figure 4.3 and this fractograph shows dimple morphology which is expected for ductile material like stainless steel.It is known that the mechanism of ductile fracture is constituted of three successive events; such as void nucleation, growth and their coalescences [45-49]. During the analysis all the facture surfaces it is concluded that the nucleation of voids in ISO/TR 15510 X12CrMnNiN17-7-5 stainless steel is created by second phase particle decohesion from the matrix. The facture surface of investigated stainless steel shows that the facture surface consists of different sizes of dimples at different places. This fact indicates that a few voids have grown substantially during fracture.

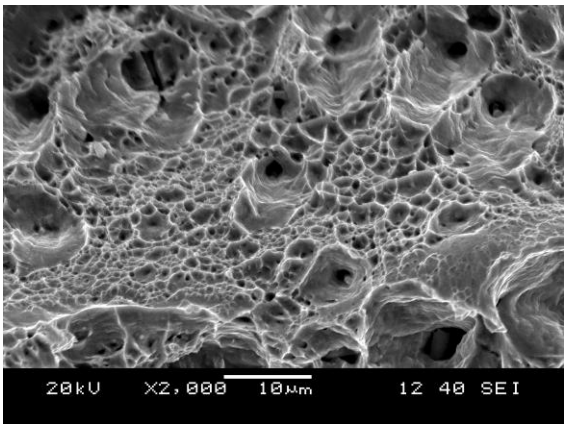

Fig.4.3: Fractographyof the broken tensile specimen.

4.5 Low cycle fatigue behavior

Low cycle fatigue tests were performed under various constant strain amplitudes at ambient temperature to characterize the fatigue properties of the material. Cylindrical specimens with the diameters of 6 mm and gauge length of 12.5 mm were used. A ±100 kN servo-hydraulic universal testing machine was used. A 12.5 mm extensometer was attached to the specimens to measure the strain during the tests. The strain-controlled tests were performed on the specimens for symmetric tension-compression strain cycles with the various strain amplitude for different strain rates up to 100 cycles. The results are shown in Figure 4.4 (a) to (h). It can be seen that the maximum stress is decreasing and minimum stress is increasing with increasing number of cycles. This phenomenon is known as cyclic softening behavior. For all the fatigue tests, similar results are obtained. Hence the non-conventional austenitic stainless steel may be treated as a cyclically soften able material.

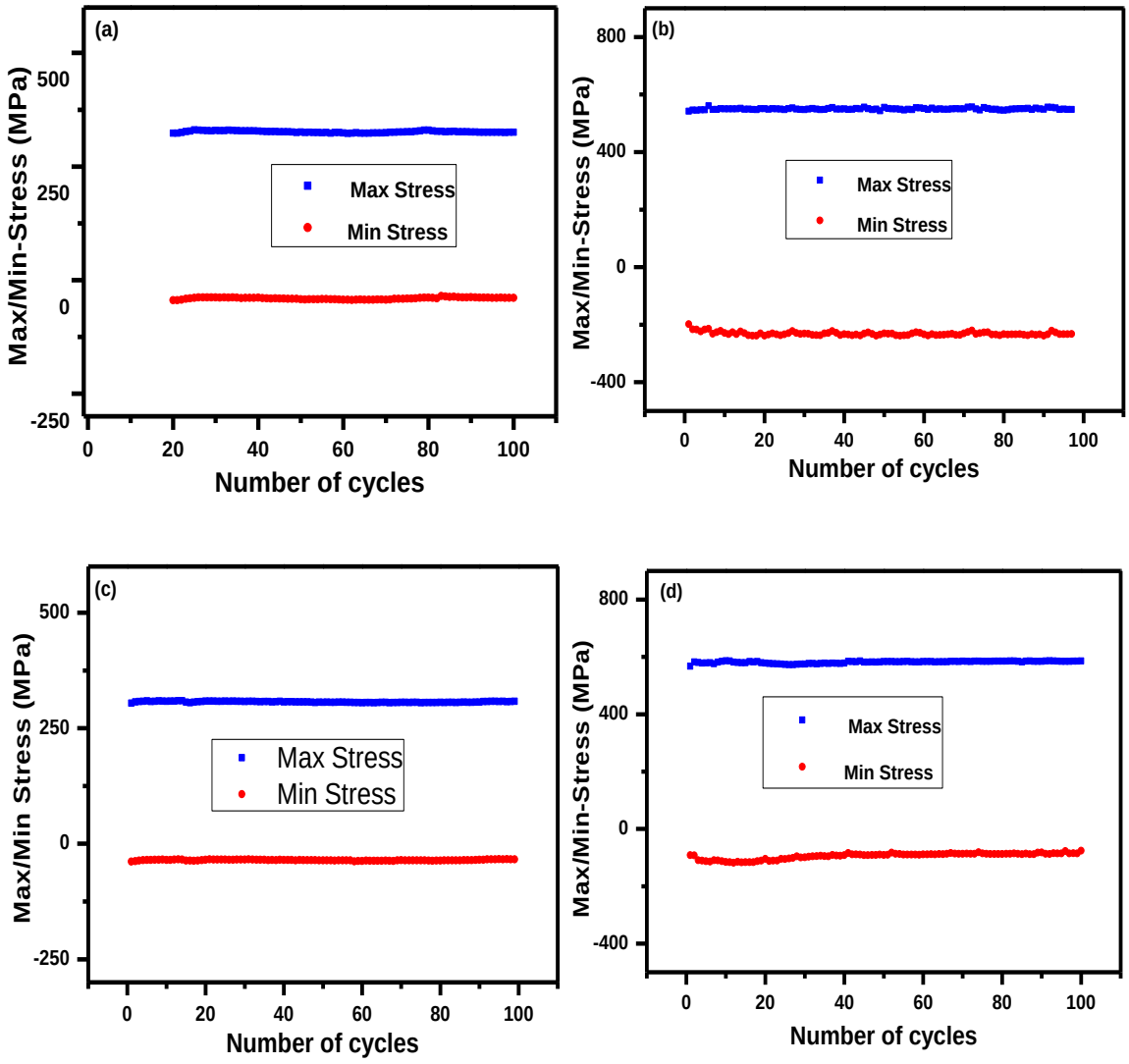

Fig.4.4: Response of maximum and minimum stress with increasing number of cycles due to various constant stain amplitude under strain control mode up to 100 cycles at ambient temperature: (a) Stain amplitude (0.10%), strain rate ($1x10^{-4}$ s^{-1}), (b)strain amplitude (0.30%), strain rate (1x10-4 s^{-1}), (c) strain amplitude (0.10%), strain rate ($5x10^{-4}$ s^{-1}), (d) strain amplitude (0.30%), strain rate ($5x10^{-3}$ s^{-1}).

Continue ……..

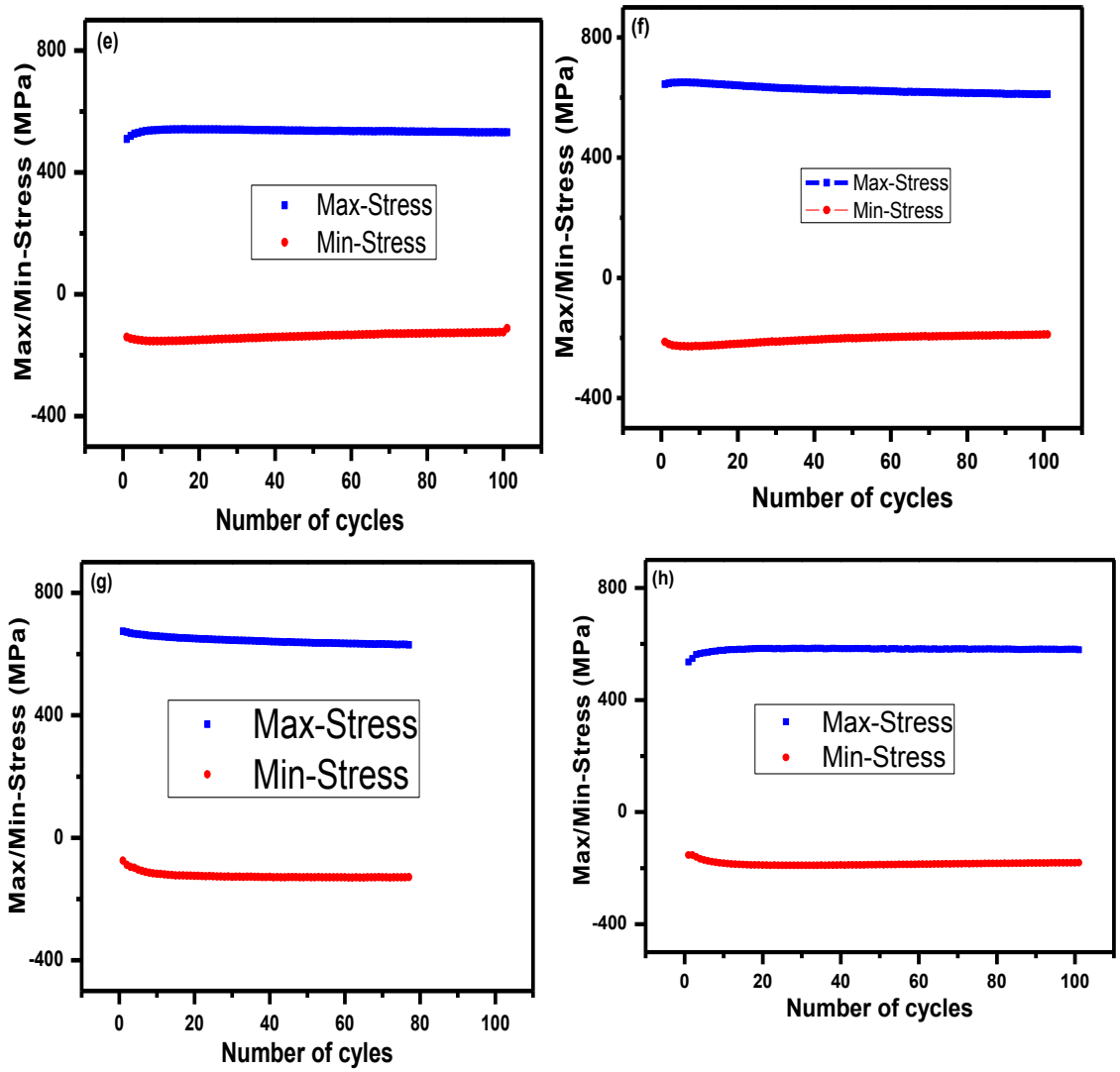

(e) strain amplitude (0.45%), strain rate (5x10-3 s^{-1}),(f) strain amplitude (0.65%), strain rate (5x10-3 s^{-1}),(g) strain amplitude (0.45%), strain rate (3x10-3 s^{-1}) (h) strain amplitude (0.65%), strain rate (3x10-3 s^{-1}).

4.6 Post fatigue tensile behavior

Post-fatigue tensile tests were conducted to examine the tensile properties of selected material subjected previous cyclic loading. Engineering stress engineering strain plots of all the specimens are shown in figure 4.5. The true stress-true strain plots are also shown here. These plots helps to determine the strain hardening coefficient values after fatigue

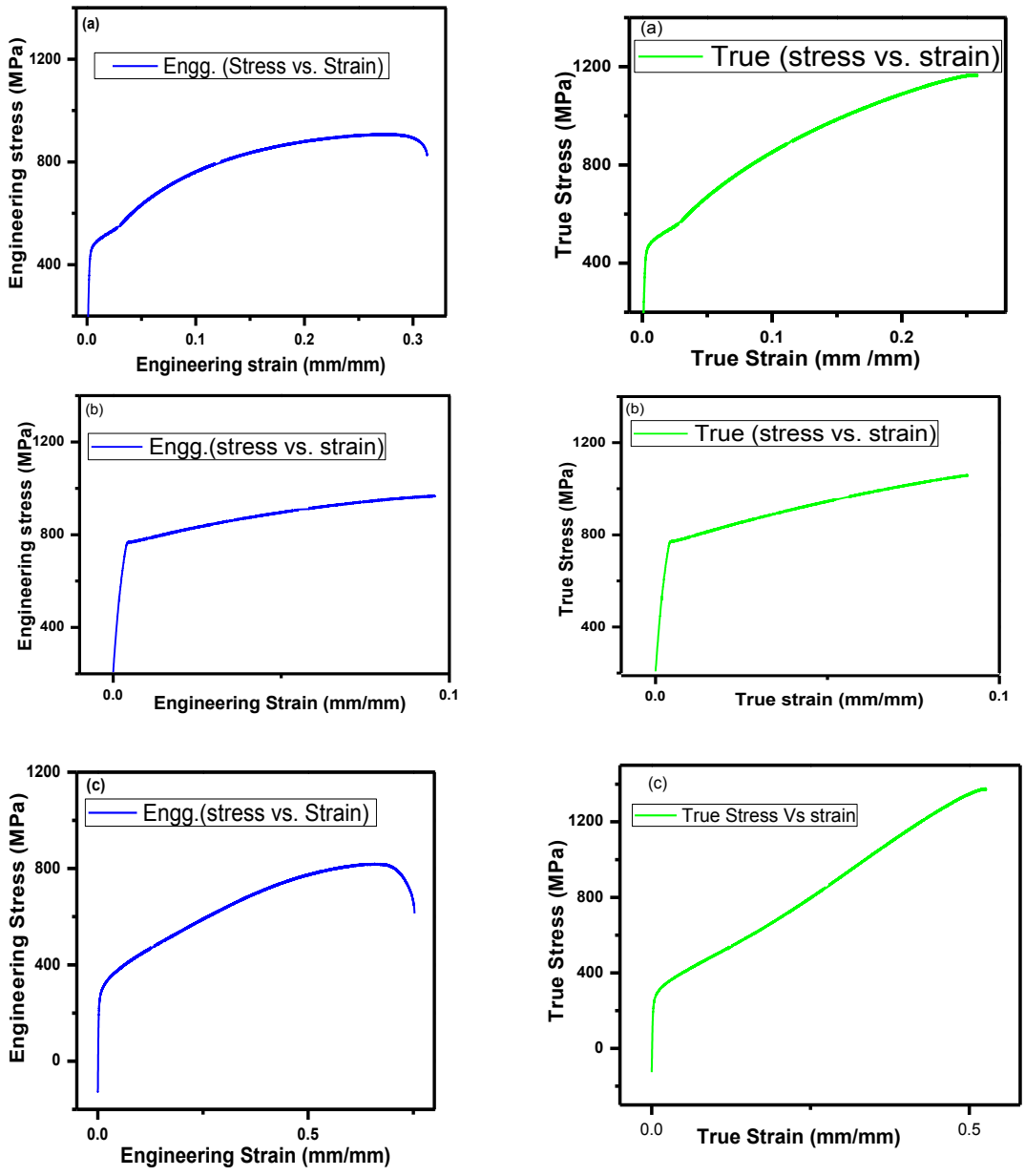

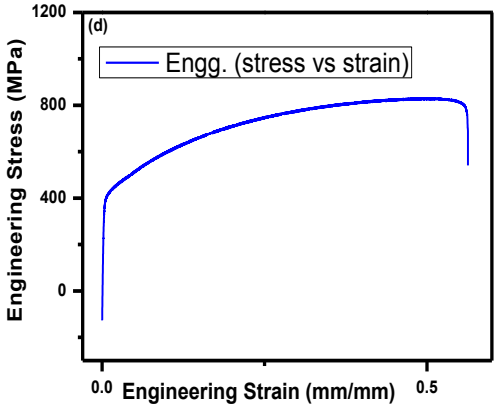
(d)
Engg. (stress vs strain)
Engineering Stress (MPa)
1200
800
400
0
0.0
Engineering Strain (mm/mm)
0.5

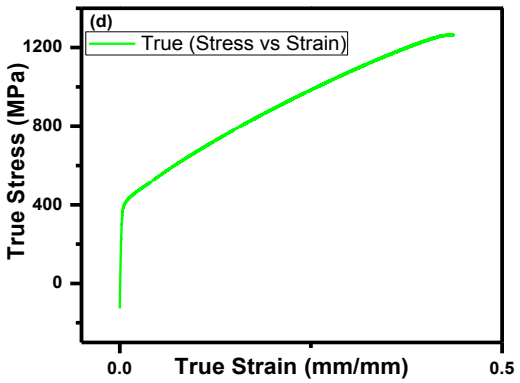
(d)
True (Stress vs Strain)
True Stress (MPa)
1200
800
400
0
0.0
True Strain (mm/mm)
0.5

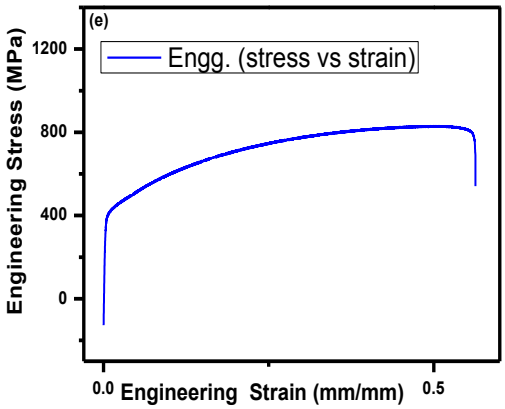
(e)
Engg. (stress vs strain)
Engineering Stress (MPa)
1200
800
400
0
0.0
Engineering Strain (mm/mm)
0.5

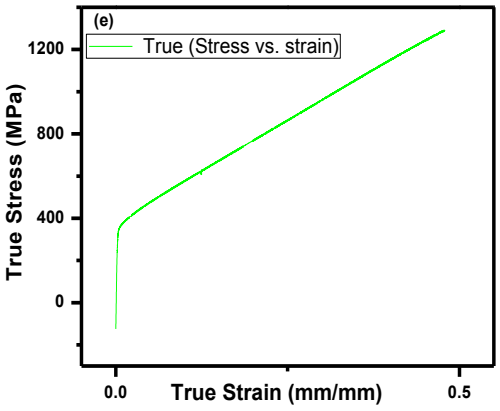
(e)
True (Stress vs. strain)
True Stress (MPa)
1200
800
400
0
0.0
True Strain (mm/mm)
0.5

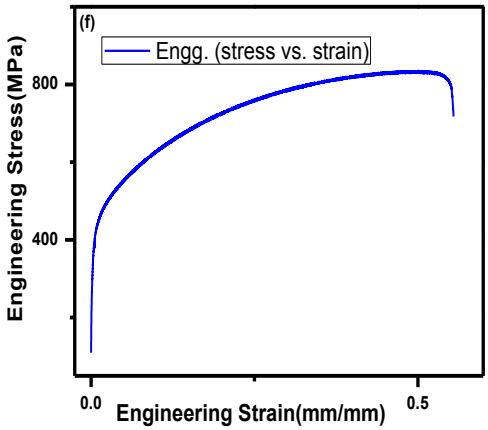
(f)
Engg. (stress vs. strain)
Engineering Stress(MPa)
800
400
0.0
Engineering Strain(mm/mm)
0.5

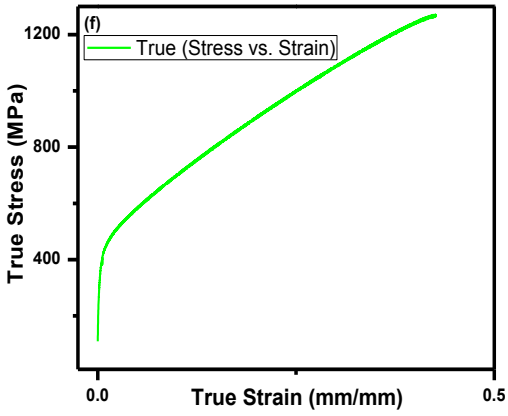
(f)
True (Stress vs. Strain)
True Stress (MPa)
1200
800
400
0.0
True Strain (mm/mm)
0.5

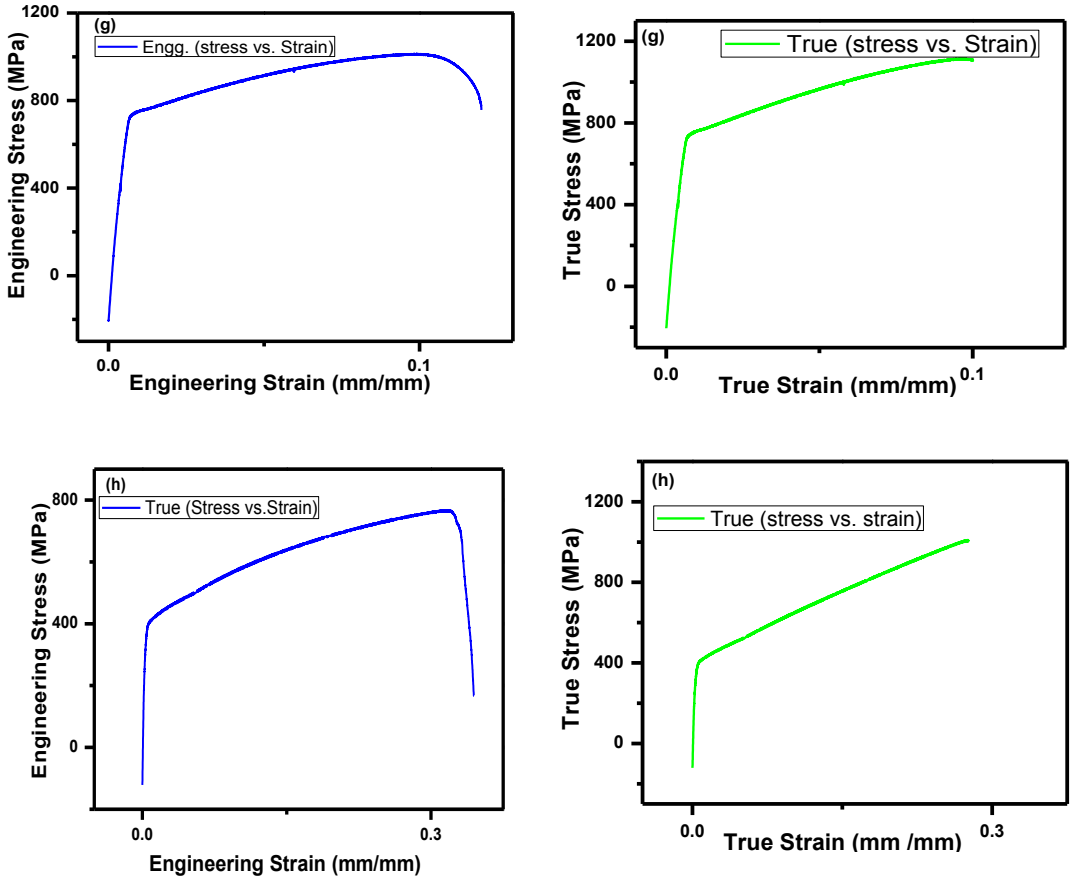

Fig.4.5: Engineering stress versus Engineering strain response and True stress versus True strain response.

The ultimate tensile strength values in the post fatigue condition for all the investigated cases are listed in Table 4.4. It can be noted that except one case, in all the cases, the tensile strength reduce in the post-fatigue condition .total percentage elongation values however, increase with reduction in strength.

Table 4.4 Post fatigue tensile properties of non conventional austenitic stainless steel.

Material: **ISO/TR 15510 X12CrMnNiN17-7-5 SS**							
Sample No.	Strain Amplitude (%)	Strain rate (s^{-1})	Frequency (Hz)	Diameter Before test (mm)	Diameter of post fatigue tensile test (mm)	UTS of post fatigue tensile test (MPa)	Total elongation percentage (e_t)
1	0.10	$1x10^{-4}$	0.025	6.12	4.38	909.24	92
2	0.30	$1x10^{-1}$	0.008	6.14	5.03	970.40	38
3	0.10	$5x10^{-4}$	0.125	6.04	4.44	820.03	80
4	0.30	$5x10^{-3}$	0.417	6.02	4.04	830.52	84
5	0.45	$5x10^{-3}$	0.278	6.06	4.72	801.37	66
6	0.65	$5x10^{-3}$	0.192	6.05	4.28	835.17	76
7	0.45	$3x10^{-3}$	0.167	6.07	4.23	1014.5	48
8	0.65	$3x10^{-3}$	0.115	6.07	5.05	767.50	54

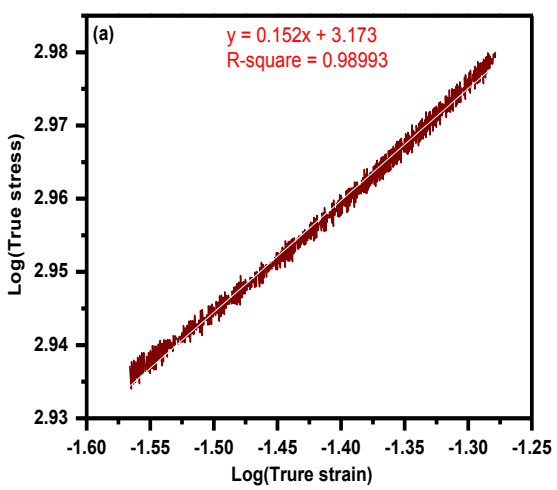

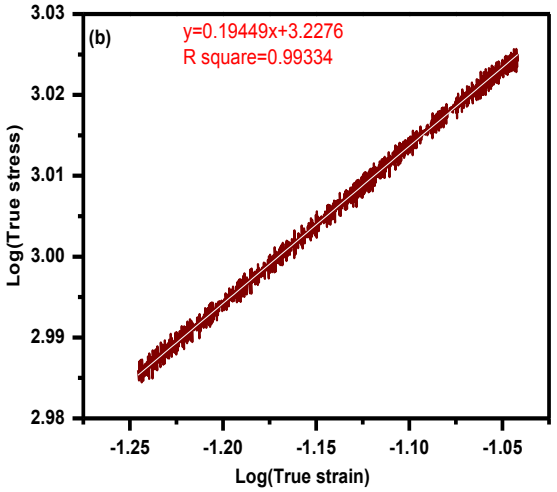

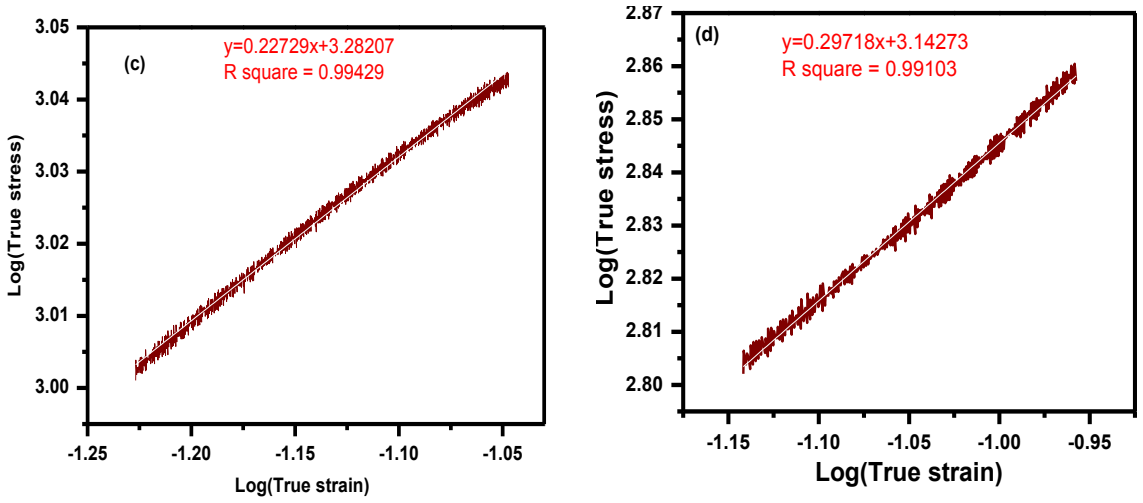

Fig 4.6: Logarithmic nature of true stress versus true strain response.

Values of strain hardening exponent *n* are calculated using Hollomon equation[38]; the results for which are given in table 4.5.

Table 4.5: Values of stain hardening and strength coefficient of post fatigue tensile tests.

Material: **ISO/TR 15510 X12CrMnNiN17-7-5 SS**		
Sample No.	Values of strain hardening exponent (*n)*	Value of strength coefficient (*K)*(MPa)
1	0.1520	1573.483
2	0.1944	1631.060
7	0.2279	1456.892
8	0.2971	1518.581

4.7 In-situ variations of Microstructure

In as-received condition the microstructure of investigated austenitic stainless steel (X12CrMnNiN17-7-5) was completely austenitic. As it is known that, the austenitic stainless steel is metastable upon monotonic and cyclicdeformation [43]. This grade of stainless steel reported that fcc phase of austenite is transformed in to bcc phase of α´ – martensite .Duyi Ye [38-42] has studied on deformation of austenite stainless steel due to low cycle fatigue tests under influence of strain amplitude and the result shows that at an intermediate strain amplitude (ε_a = 0.9%)the martensitic phase appeared as thin parallel individualstriations in the austenitic grains. There is lack of literature on influence of tensile deformation after low cycle fatigue loading on microstructural variation of special grade of austenitic stainless steel. Therefore, to understand its influence on microstructural variation of X12CrMnNiN17-7-5 austenitic stainless steel X-ray diffraction analyses have been carried out which shows α´– martensite phase present in the diffraction pattern shown in figure 4.7. Intensity relatives to its peak observed by X-ray diffraction analysis given in table 4.6, and the increasing percentage of martensite due to increasing strain amplitude during fatigue test shown in figure 4.8

Fig.4.7 X-ray diffraction analyses due to combined effects of fatigue and tensile loading.

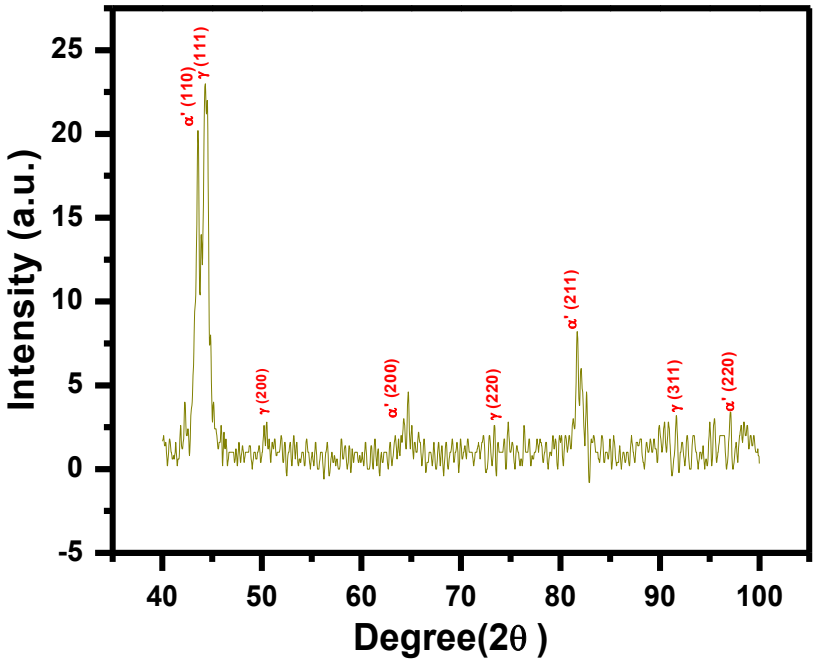

Table 4.6: Intensity and planes relatives to its peak observed by X-ray diffraction analysis and volume fraction of deformed martensite .

Material:**ISO/TR 15510 X12CrMnNiN17-7-5 SS**				
Peak No.	Degree (2 Theta)	Intensity(a.u.)	Planes	Phases
1	43.56	1	(110)	ά -martensite (BCC)
8	65.93	2	(200)	
13	81.8	7	(211)	
20	98.8	3	(220)	
2	44.52	23	(111)	γ austenite (FCC)
4	50.42	3	(220)	
10	76.47	1	(200)	
17	98.77	3	(311)	

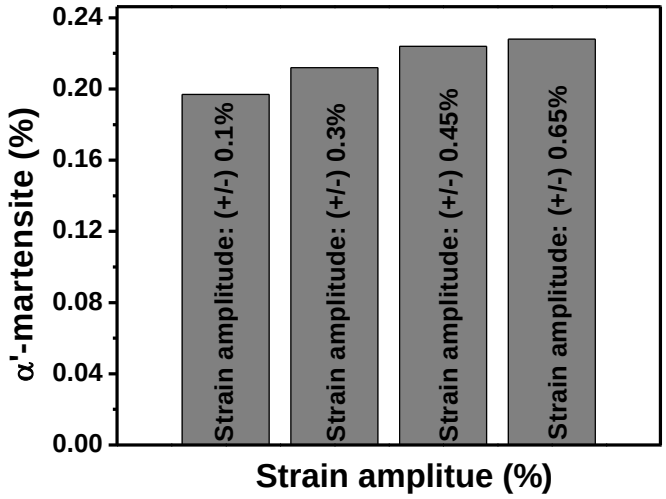

Fig.4.8: Histogram showing variation of percentage of martensite due to increasing percentage of total strain amplitude of fatigue loading.

CHAPTER 5

Conclusions and Scope for Future Research

Conclusions

The obtained results related to low cycle fatigue and post fatigue behavior of ISO/TR15510 X12CrMnNiN17-7-5 stainless steel and its micro structural variation due to its plastic deformation.

1. The results of low cycle fatigue experiments indicate that the investigated material cyclically softens during all the employed fully reversed strain controlled tests.

2. Results of post fatigue tensile tests indicate that the ultimate tensile strength of the material decreases as compared to its initial tensile strength (i.e. in solution annealed condition) values; the ductility, on the other hand, increases with reduction in strength.

3. The results of X-ray diffraction analyses indicate that phase transformation takes place during cyclic loading; parent austenite phase transforms to deformed martensite. The volume fraction of martensite increases as strain amplitude of fatigue loading is increased.

Scope for future research

1. The investigation of micro-mechanism associated with low cycle fatigue and post fatigue tensile deformation can be done using TEM.

2. The cyclic response of material at different strain amplitude under various temperatures during low cycle fatigue test and its effect on material tensile properties can be observed.

References

[1] Egor P. Popov, Engineering Mechanics of Solids, Sweden, Prentice Hall PTR,1989.

[2] Kanazawa, K., Yamaguchi, K., and Nishijima, S., Mapping of low cycle fatigue mechanisms at elevated temperatures for an austenitic stainless steel, ASTM special technical publication, no942(1988):pp. 519-530.

[3] Coles, A., Hill, G. I., Dawson, R. A. T., and Watson, S. J., International Conference on Thermal and High Strain Fatigue, Institute of Metals, London,.32 (1967):pp. 270-294.

[4] Campbell, R. D., Journal fi-Engineering for Industry, Transactions of American Society of Engineers. 93(1971): pp. 887-892.

[5)] Coffin, L. F. M, Corrosion Fatigue, National Association of Corrosion Engineers, Texas, NACE-2(1972): pp. 590-600.

[6] Wareing, J., Tomkins, B., and Sumner, G., Fatigue at Elevated Temperatures, American Society for Testing and Materials (ASTM), STP 520(1973):,pp. 123-138.

[7] Yamaguchi, K. and Kanazawa, K., Metallurgical Transactions,American Society for Metals and the Metallurgical Society of AIME, 11A(1980):,pp. 1691-1699.

[8] Nishiyama Z, Martensitic transformation, Materials science and technology, New York , 2nd edition: Academic Press, 1978.

[9] Albert W. A. J., observations of metal fatigue, German mining administrator, 30(1836): pp. 2-4

Reference

[10] Ellyin, F., Fatigue Damage, Crack Growth and Life Prediction, London(UK) Chapman&Hall, (1997).

[11] Dieter, G. E., Mechanical Metallurgy, Singapore, McGraw-Hill Book Company, (1987).

[12] Golub V. P. , Kryzhanovskii V. I. , and Pogrebnyak A. D., Fatigue strength of metallic and composite materials under repeated tension–compression, International Applied Mechanics, 42 (2006). PP. 40–50.

[13] Beer F. P., Johnston E. R., Mechanics of Materials. New York, McGraw-Hill, 1992.

[14] Mitchell MR.,Fundamentals of modern fatigue analysis for design, ASM International; 39 (1996): pp. 229–49.

[15] Manson S.S.,Fatigue: a complex subject – some simple approximation, Experiment Mechanical, 5(1965): pp.193–226.

[16] Coffin L.F., A study of the effect of cyclic thermal stresses on a ductile Metal.Trans ASME, 76(1954): pp. 931–50.

[17] Basquin O.H., The exponential law of endurance tests, Am Soc Test Mater Proc, 10 (1910): pp. 625–30.

[18] Berger C, Kaiser B., Results of very high cycle fatigue tests on helical compression springs, International Journal Fatigue , 28(2006): pp.1658–63.

Reference

[19] Sonsino C.M., Course of SN-curves especially in the high-cycle fatigue regime with regard to component design and safety, International Journal Fatigue, 29(2007): pp. 2246–58.

[20] Coffin L.F.,A note on low cycle fatigue laws, J Mater JMLSA 6(2) (1971): pp. 388–402.

[21] Shimada K, Komotori J, Shimizu M., The applicability of the Manson–Coffin law and Miner's law to extremely low cycle fatigue., Trans JpnSocMechEng A., 53(491) (1987): pp. 1178–85.

[22] Komotori J., Shimizu M., Fracture mechanism of ferritic ductile cast iron in extremely low cycle fatigue.,Elsevier Science Ltd.;39 (1998): pp. 39–44.

[23] Chung Y.S, Abel A., Low cycle fatigue of some aluminium alloys., ASTM STP 942, American Society for Testing and Materials(ASTM), 942(1988): pp. 94–106.

[24] Kanvinde A.M., Deierlein G.G., Continuum based micro-models for ultra low cycle fatigue crack initiation in steel structures., Forensic Engineering Symposium, 19(171) (2005): pp. 20–4.

[25] Hatanaka K, Fujimitsu T., Some considerations on cyclic stress–strain relation and low cycle fatigue life., Trans JpnSocMechEng A., 50(451) (1984): pp. 291–300.

[26] Kuroda M., Extremely low cycle fatigue life prediction based on a new cumulative fatigue damage model. International Journal Fatigue, 24(6) (2002): pp.699–703.

[27] Tateishi K., Hanji T., Minami K., A prediction model for extremely low cycle fatigue strength of structural steel., International Journal Fatigue, 29(5)(2007): pp. 887–96.

[28] Chen Y.J., Liu Y.H., Xie L.Y., Power exponent function model for low-cycle fatigue life prediction and its applications Part I: Models and validations., International Journal Fatigue , 29(1)(2007): pp. 1–9.

[29] Zhou Y., Ou Y.C., Lee G.C and Connor JS.O.,A Pilot Experimental Study on the Low Cycle Fatigue Behavior of Stainless Steel Rebars for Earthquake Engineering Applications,University at Buffalo,(2008): pp. 1-4.

[30] The encyclopaedia, (may2014), 05224G, Chapter 14 the fatigue, pp. 251.

[31] Halama R., Sedlák J.,and Šofer M.,Numerical Modelling, Phenomenological Modelling of Cyclic Plasticity,In Tech,(2012).

[32] Rice R.C., Leis B.N., Berns H.D., Nelson D.V., Lingenfleser D, Mitchell MR., Fatigue design handbook, Warrendale, Tensile Testing ASM International, 2004.

[33] Bagliona L.D, Mendeza J.,Low cycle fatigue behavior of a type 304L austenitic stainless steel in air or in vacuum, at 20°C or at 300°C: relative effect of strain rate and environment,Procedia Engineering ,2(2010): pp. 2171-2179.

[34] Gerland M., Alain R., Saadi B.A., Mendez J.,Low cycle fatigue behaviour in vacuum of a 316L-type austenitic stainless steel between 20 and 600 degrees C.2. dislocation structure evolution and correlation with cyclic behaviour., Materials Science and Engineering a-Structural Materials Properties Microstructure and Processing , 229(1-2) (1997): pp. 68-86.

[35] Yong J.O., Hwang T.B.,and Shin B.M., Division of Advanced Materials Engineering, Korea Materials Transactions(The Japan Institute of Metals), 46No. 2 (2005): pp. 317- 322.

[36] Srinivasan V.S., Valsan M.,Sandhya R.,RaoK.B.S, Mannan S.L., Sastry D.H., High temperature time-dependent low cycle fatigue behaviour of a type 316L(N) stainless steel ,International Journal of Fatigue, 21 (1999): pp. 11–21.

[37] Solomon N., and Solomon l., Deformation induced martensite in AISI 316 stainless steel rev. metal. Madrid, 46 (2) (2010): pp. 121-128.

[38] De, A. K., Murdock D. C., Mataya M.C., Speer J. G., and Matlock D. K., Quantitative measurement of deformation-induced martensitein 304 stainless steel by X-ray diffraction, Scripta Materialia, 50(2000): pp. 1445–1449.

[39] Nayar A.,The steel hand book, New york city,Tata MC Graw-Hill company Limited., 1997.

[40] Hecker, S.S., Stout M.G., Staudhammer. K.P., and Smith J.L.,(1982),Effects of strain state and strain rate on deformation-induced transformation in 304 stainless steel., Metall. Mater. Trans. A, 13A (1982): pp. 619–626.

Reference

[41] E., Standard Test Methods for Determining Average Grain Size,
Annual Book of ASTM Standards, Philadelphia, PA.,ASTM, 03.01(2004): pp. 112-04.

[42] Standard Test Methods for Tension Testing of Metallic Materials,
Annual Book of ASTM Standards, Philadelphia, PA., ASTM, 03.01(2008): pp. E8M-08.

[43] ASM International Handbook Committee ,Stainless Steels, ASM Specialty Handbook, ASM International, Ohio.1999.

[44] Standard Test Methods for Determining Average Grain Size,
Annual Book of ASTM Standards, Philadelphia, PA., ASTM, 03.01(2004): pp.E 112-0.

[45] Tvergaard V.,Ductile fracture by cavity nucleation between larger voids,
Journal of Mechanics and Physics of Solids, 30(1982): pp. 265–286.

[46] ASM International Handbook Committee Stainless Steels, ASM Specialty Handbook, ASM International, Ohio, (1999).

[47] Thomason, P. F,ductile fracture by the growth and coalescence of
microvoids of non-uniform size and spacing, Actametall, mater. 41No. 7(1993), pp. 2127-2134.

[48] Tvergaard, V.,Ductile fracture by cavity nucleation between larger voids,
Journal of Mechanics and Physics of Solids, 30No.4(1982): pp. 265–286.

[49] Bandstra J.P., Koss. D.A ,Modeling the ductile fracture process of void coalescence by void-sheet formation, Materials Science and Engineering
A, 319–321(2001): pp. 490–495.